

# Observation of modified radiative properties of cold atoms in vacuum near a dielectric surface

V. V. Ivanov, R. A. Cornelussen, H. B. van Linden van Heuvell, and R. J. C. Spreeuw\*

*Van der Waals-Zeeman Institute, University of Amsterdam,  
Valckenierstraat 65, 1018 XE Amsterdam, The Netherlands*<sup>†</sup>

(Dated: December 2, 2024)

We report on measurements of the radiative properties of cold  $^{87}\text{Rb}$  atoms close to a dielectric-vacuum interface. This is the first observation of a quantum electrodynamic (QED) modification of radiative properties in vacuum near a dielectric surface. A cloud of cold atoms was created using a magneto-optical trap (MOT) and optical molasses cooling. Evanescent waves (EW) were used to observe the behavior of the atoms near the surface. We observed an increase of the natural linewidth with up to 25% with respect to the free-space value. We attribute this to QED broadening and level shifts, as well as local Stark shifts near the surface. By varying the characteristic EW length we have observed a position dependence characteristic for QED.

PACS numbers: 42.50.-p, 42.50.Xa

Keywords: Vacuum field fluctuations, cold atoms, spontaneous emission

## I. INTRODUCTION

An electronically excited atom (or molecule) can decay to the ground state by spontaneous emission. The characteristic rate at which this occurs is not simply an intrinsic property of the atom but also depends on the environment. The spontaneous emission rate is proportional to the density of electromagnetic field modes (DOS, or “density of states”), which is determined by the electromagnetic boundary conditions. The DOS can thus be modified, and with it the spontaneous emission rate. The boundary conditions imposed by the environment not only change the radiative linewidth but also induce energy level shifts and thus change the transition frequencies. These include the electrostatic or Van der Waals shift, the Casimir-Polder shift (modification of the Lamb shift), and resonant radiative shifts. For a review see, e.g. Ref. [1].

Modified spontaneous emission was first observed by Drexhage [2, 3], using dye monolayers separated from an interface by fatty acid layers. Both inhibited and enhanced spontaneous emission have since then been observed by others in a variety of geometries and circumstances [4, 5, 6, 7]. Remarkably, the radiative linewidth of an atom *in vacuo* at a distance of the order of an optical wavelength from a dielectric surface has never been investigated experimentally. Energy level shifts have been studied for atom inside cavities [8, 9] and in vapor cells, using selective reflection spectroscopy [10, 11]. The situation of an atom in front of a distant mirror has recently been investigated using a single trapped ion. Both the broadening of the radiative linewidth and energy level shifts have been reported for this system [12, 13].

In this paper we experimentally investigate the radia-

tive properties of cold ( $T \approx 10 \mu\text{K}$ ) atoms of  $^{87}\text{Rb}$  close to a glass surface, at a distance on the order of an optical wavelength. Using our method of evanescent-wave spectroscopy [14] we have observed linewidth broadening with contributions from both QED broadening and level shifts.

## II. METHOD: EVANESCENT-WAVE SPECTROSCOPY

The radiative linewidth  $\Gamma$  is proportional to the power spectral density of the vacuum field fluctuations at the position of the atom [15], i.e. the local DOS. The proximity of a dielectric surface imposes a boundary condition on the field, changing the DOS. This leads to a modification of  $\Gamma$  and to energy level shifts [7, 10, 11, 15, 16, 17, 18]. Both the linewidth broadening and the level shifts are significant mainly at distances  $z \lesssim \lambda = \lambda/2\pi$ , where  $\lambda$  is the wavelength of the dominant electronic transition. In our case this is the  $D_2$  resonance line of Rb, and  $\lambda = 124 \text{ nm}$ .

Therefore we probe the cold atoms near the glass surface using evanescent-wave (EW) spectroscopy [14]. This method is selectively sensitive to atoms very close to the surface. An EW appears when our probe beam undergoes total internal reflection at the glass surface with index of refraction  $n = 1.51$ , see Fig. 1. The optical field on the vacuum side decays exponentially with the distance  $z$  to the surface,  $E(z) \propto \exp(-z/\xi)$ . Atoms can absorb light from the EW, if their distance to the surface is on the order of the decay length  $z \lesssim \xi \sim \lambda$ . The decay length can be adjusted by changing the angle of incidence  $\theta$  according to  $\xi(\theta) = \lambda(n^2 \sin^2 \theta - 1)^{-1/2}$ . By adjusting  $\theta$  we can thus vary the distance scale at which the atoms interact with the probe light. By increasing  $\theta$  further above the critical angle  $\theta_c = \arcsin n^{-1}$ , the absorption will occur closer to the surface, where  $\Gamma$  is more strongly modified.

For atoms in free space, the absorption profile is given

\*Electronic address: spreeuw@science.uva.nl

<sup>†</sup>URL: <http://www.science.uva.nl/research/ap1p/>

by a Lorentzian profile, centered at the (free-space) atomic transition frequency  $\omega_{eg} = c/\lambda$  and with a full width at half maximum (FWHM) equal to the natural linewidth  $\Gamma_\infty/2\pi = 6.07$  MHz. Both quantities change in the proximity of the surface, as will be described below. Roughly speaking these  $z$ -dependent Lorentzians become convoluted with the EW energy density  $U(z) \propto \exp(-2z/\xi)$ . We expect the width of the resulting absorption profile to increase with the angle of incidence  $\theta$ . In the experiment we measured this by tuning an EW probe laser across the profile and measuring the absorption.

### III. EXPERIMENT

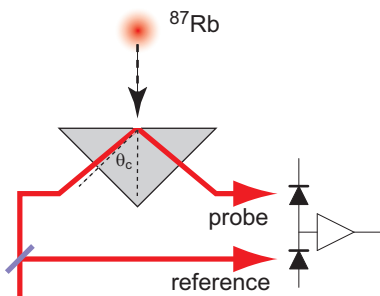


FIG. 1: Scheme of the experiment. A weak evanescent-wave probe beam is reflected from the prism surface and collected on a photodiode. The reference beam has equal power but bypasses the vacuum cell. The difference photocurrent of probe and reference beams yields the absorption signal, typically a fraction of  $10^{-3} - 10^{-4}$  of the probe. A second reference beam (not shown) was used to monitor variations in the probe power. We also collect the fluorescence from the MOT to normalize for shot to shot variations of the number of atoms.

The major part of our experimental setup has been described previously [19]. We produced clouds of cold  $^{87}\text{Rb}$  atoms using magneto-optical trapping inside a ultra high vacuum cell (base pressure  $p \simeq 10^{-10}$  mbar). After postcooling in optical molasses we ended up with about  $3 \times 10^7$  atoms, at a temperature of  $9 \mu\text{K}$ . At this temperature the Doppler width is 90 kHz (FWHM). The cooling lasers were then switched off and the atoms fell down toward the surface of a glass prism, about 3.6 mm below. The center of the cloud reached the prism surface and the EW spot after 27 ms. Just before hitting the surface, the atoms briefly interact with a weak,  $p$ -polarized, EW probe beam, see Fig. 1. The intensity of the probe was kept well below the saturation intensity to avoid power broadening. Using  $0.35 \mu\text{W}$  and a waist of about 1 mm, the maximum saturation parameter was  $s \simeq 0.08$ .

The probe beam was derived from a home-built diode laser system, locked to the  $F = 2 \rightarrow F' = (1, 3)$  crossover resonance in the  $D_2$  line of  $^{87}\text{Rb}$  (780 nm). We used an acousto-optic modulator (AOM) to shift the probe frequency near resonance with the  $F = 2 \rightarrow F' = 3$

transition and to tune it across the resonance. Before sending it into the cell, a fraction of the probe beam was split off and sent to a photodiode as a reference. After total internal reflection on the prism surface the probe beam was focused on a second photodiode. The photocurrents of the two photodiodes were subtracted to obtain our signal, typically a fraction of  $10^{-3} - 10^{-4}$  of the probe.

The difference photocurrent was amplified by a low-noise current amplifier (Femto, LCA-100K-50M, 50 MV/A transimpedance) and sent through a low-pass filter ( $RC = 1$  ms) to further reduce the noise. All photodiode signals, including a power monitor and a MOT fluorescence monitor were acquired using a digital storage oscilloscope. The latter two signals were used to normalize the absorption signals for variations in the probe power and shot-to-shot variations in the number of cold atoms.

In Fig. 2 we show a typical EW absorption time trace with the probe beam tuned near resonance, for an angle of incidence  $\theta_i = \theta_c + 0.52^\circ$ . The signal has been averaged  $100 \times$  to reduce the noise. Without filtering, the absorption signal has a Gaussian shape due to the velocity distribution of the falling atoms. However, in order to suppress slow drifts in the difference photocurrent we used AC coupling (i.e. a high-pass filter) on the oscilloscope. As a result the Gaussian signal has been distorted. Furthermore it is superposed on an exponentially decaying transient originating from switching on the probe beam.

The position of the peak corresponds to the fall time of the atoms. The width is given by the ratio of the size ( $\sim 3$  mm) and velocity ( $\sim 0.3$  m/s) of the atom cloud as it reaches the surface. The height of the peak is  $\sim 2$  mV, which corresponds to an absorbed power of  $\sim 80$  pW. The time-integrated signal amounts to  $\sim 3 \times 10^6$  absorbed photons, or  $\sim 2$  scattered photons per atom in the center of the EW. If we tune the probe laser away from resonance, or increase the angle of incidence, the signal amplitude decreases and the number of scattered photons drops to much less than one per atom. Eventually the signal disappears in the noise, which is dominated by shot noise.

### IV. DATA PROCESSING

Despite the signal distortion, we can extract the amplitude and width of the original Gaussian by fitting the known shape of the filtered time trace. We took the fitted height of the Gaussian as the measure for the amount of absorption. The Gaussian width is essentially constant. Thus, the height of the peak is proportional to the absorbed EW power, which depends on the EW detuning and the angle of incidence.

For a given angle of incidence we measured time traces for different detunings of the EW probe. The fitted Gaussian height as a function of probe detuning yields an ab-

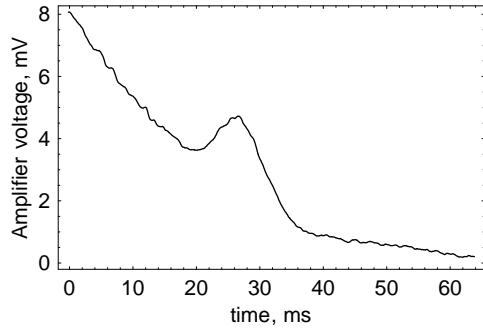


FIG. 2: A typical time-of-flight signal taken with the evanescent-wave probe beam (100 $\times$  average). The peak around 27 ms is due to the absorption of evanescent probe light by cold atoms arriving at the surface. As a result of high pass filtering the signal has been distorted and sits on top of an exponentially decaying transient (1/e time 26 ms).

sorption profile as shown in Fig. 3. From this we extracted a Lorentzian line width by fitting a Voigt profile

$$\mathcal{V}(\omega) = \frac{A}{\sqrt{2\pi}\Delta} \text{Re} \left\{ \exp \left[ - \left( \frac{\omega - \omega_{eg} + i\Gamma/2}{\sqrt{2}\Delta} \right)^2 \right] \times \text{erfc} \left( -i \frac{\omega - \omega_{eg} + i\Gamma/2}{\sqrt{2}\Delta} \right) \right\}, \quad (1)$$

where  $A$  is an amplitude and  $\text{erfc}(\cdot)$  is the complementary error function. This Voigt profile is the convolution of a Gaussian with a fixed width  $\Delta/2\pi = 1$  MHz and a Lorentzian with variable width  $\Gamma$ .

The fixed Gaussian linewidth accounts for the finite spectral width of the probe laser. Our grating stabilized diode laser system has a spectral linewidth comparable to the observed atomic linewidth broadenings [20, 21]. We determined the laser linewidth in a separate experiment by observing the beat note between two similar but independently locked diode lasers on a photodiode. The observed decoherence of the beat signal was well described by a Gaussian with a width of 1 MHz. This is the linewidth at short (ms) time scales. For longer timescales we rely on the feedback loop of the laser locking electronics.

The Lorentzian linewidth  $\Gamma$  contained in the Voigt profile is a fit parameter. We performed measurements of the absorption profile several times for two different angles of incidence ( $\theta - \theta_c = 0.16^\circ$  and  $0.52^\circ$ ). For each absorption profile we find one value for  $\Gamma$ . The results are shown in Fig. 4. For larger angles, the absorbed power became too small compared to the noise, due to the decreasing EW volume. The vertical error bars in Fig. 4 are entirely determined by the scatter of the datapoints as seen in Fig. 3.

In the limit of large EW decay length, or  $\theta \rightarrow \theta_c$ , we expect  $\Gamma$  to tend to the free-space value  $\Gamma_\infty$ . Unfortunately, at angles very close to the critical angle,  $\theta - \theta_c < 0.05^\circ$ , the probe beam cannot be treated as a plane wave due to

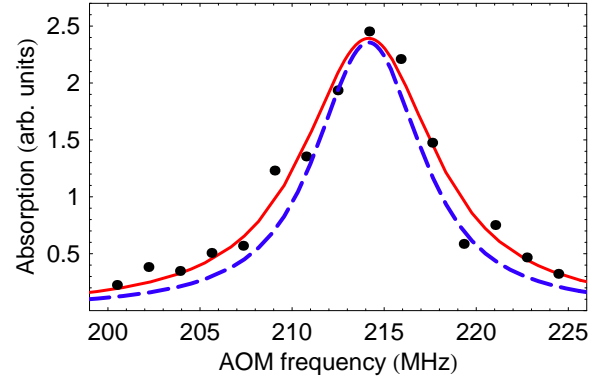


FIG. 3: Measured and fitted absorption profiles. The AOM frequency is the shift imparted to the frequency of the locked probe laser to tune it near resonance. Each data point is the fitted Gaussian amplitude of a 100 $\times$  averaged time trace as in Fig. 2. The solid line is the fitted Voigt profile. For comparison, the dashed line shows the free-space Lorentzian profile.

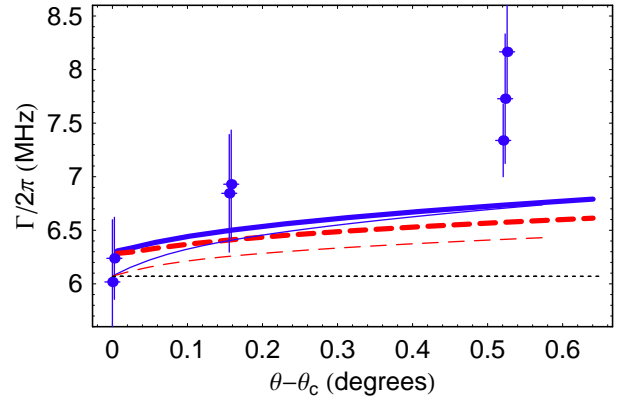


FIG. 4: (Color online) Fitted linewidths for varying angle of incidence of the evanescent-wave (EW) probe. The data points at  $\theta - \theta_c = 0$  have been measured in free space, instead of with an EW probe. The thin lines are the calculated widths based on Eq. (8), the thick lines based on an integration of the optical Bloch equations (see text). The red dashed curves show the result when level shifts are not taken into account, the blue solid curves take into account both broadening and level shifts.

the finite diffraction angle. In order to avoid this complicated situation, we performed an independent check by measuring the linewidth in free space. The same probe laser was used to measure the absorption by the atomic cloud while falling, at a height of 2 mm above the surface. A short flash of probe light was recorded on a CCD camera. The detuning was varied in a similar way as in the EW probe measurements. The linewidth was again determined by fitting a Voigt profile. We plotted this free-space value in Fig. 4 as the datapoint for  $\theta - \theta_c = 0$ .

## V. THEORY FOR $\Gamma(z)$

We will now compare the measured  $\theta$ -dependence of the linewidth to QED calculations. When the atom approaches the dielectric surface, both the radiative linewidth  $\Gamma$  and the resonance frequency  $\omega_{eg}$  change in a  $z$ -dependent way. The latter also appears as a broadening in the experiment because the evanescent wave performs an integration over  $z$ .

The absorption from the EW probe beam can be calculated by performing a spatial integration of the photon scattering rate over the vacuum half space  $z > 0$ . The photons that are scattered out of the EW by atoms are missing from the reflected probe beam so that the reflectivity drops below unity. This approach works well if the absorption is small ( $\ll 1$ , i.e. no probe depletion). In the limit of low saturation the photon scattering rate is  $\Gamma(z)s(z)/2$ , with the saturation parameter given by

$$s(z) = \frac{cU(z)}{I_0} \frac{\Gamma_\infty^2/4}{\delta^2(z) + \Gamma^2(z)/4}, \quad (2)$$

where  $U(z) \propto \exp(-2z/\xi)$  is the EW energy density and  $I_0 = 1.6 \text{ mW/cm}^2$  is the (free space) saturation intensity. Note that an increase of  $\Gamma(z)$  not only increases the Lorentzian width but also multiplies into the photon scattering rate, thus increasing the on-resonance rate. This effect tends to favor the detection of atoms near the surface.

The modification of the radiative linewidth of an atom near a plane dielectric surface has been described theoretically in terms of dipole damping rates  $\Gamma_\perp$  and  $\Gamma_\parallel$  [15, 17]. The subscripts ( $\perp, \parallel$ ) refer to dipoles oriented perpendicular and parallel to the surface, respectively. The dipole damping rates vary with the distance to the surface  $z$ , in the notation of Ref. [17] (note also [26]):

$$\frac{\Gamma_\perp(z)}{\Gamma_\infty} = 1 + \frac{3}{2} \text{Re} \int_0^\infty \frac{u^3 r^p(u) du}{\sqrt{1-u^2}} \exp(2ikz\sqrt{1-u^2}), \quad (3)$$

$$\frac{\Gamma_\parallel(z)}{\Gamma_\infty} = 1 + \frac{3}{4} \text{Re} \int_0^\infty \frac{u du}{\sqrt{1-u^2}} (r^s(u) + (u^2 - 1)r^p(u)) \times \exp(2ikz\sqrt{1-u^2}). \quad (4)$$

Here  $k = 2\pi/\lambda$ , and  $r^p(u)$  and  $r^s(u)$  are the Fresnel reflection coefficients for  $p$  and  $s$  polarization:

$$r^p(u) = \frac{n^2\sqrt{1-u^2} - \sqrt{n^2-u^2}}{n^2\sqrt{1-u^2} + \sqrt{n^2-u^2}}, \quad (5)$$

$$r^s(u) = \frac{\sqrt{1-u^2} - \sqrt{n^2-u^2}}{\sqrt{1-u^2} + \sqrt{n^2-u^2}}. \quad (6)$$

In our experiment we probe  $^{87}\text{Rb}$  atoms on the transition  $5S_{1/2}(F=2) \rightarrow 5P_{3/2}(F'=3)$ . An atom in the excited magnetic hyperfine state  $|F', m_F\rangle = |3, m\rangle$  can decay to the ground state  $|2, m-q\rangle$  with  $q = 0, \pm 1$ .

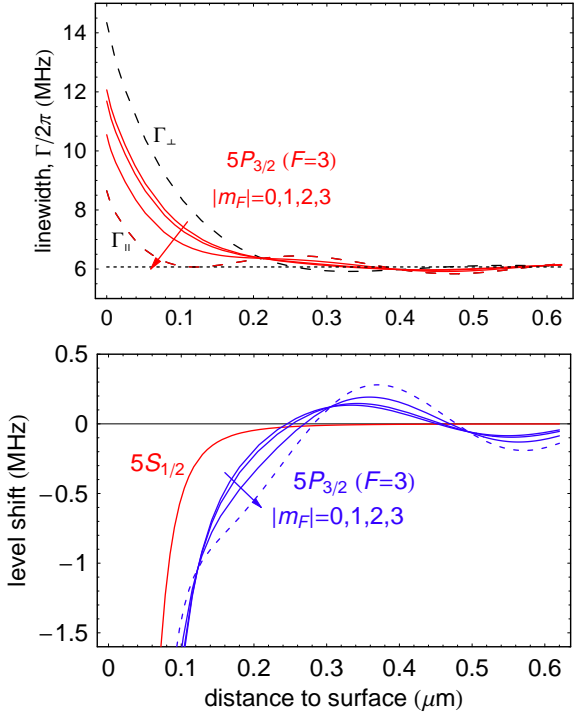


FIG. 5: Distance dependence of line widths (upper) and level shifts (lower) of the relevant hyperfine magnetic sublevels. In the upper graph, the dashed curves show the dipole damping rates, see Eqs. (3, 4). The curves for the  $F = |m_F| = 3$  states coincide with that for  $\Gamma_\parallel$  and do not contribute in the experiment. The dotted line is the free-space value. In the lower graph the level shifts of the  $F = |m_F| = 3$  states do not contribute and are again shown as dashed.

Choosing the quantization axis perpendicular to the surface, the  $q = 0$  decay channel is governed by  $\Gamma_\perp$ , the  $q = \pm 1$  channels by  $\Gamma_\parallel$ . The decay rate for a given sublevel  $|3, m\rangle$  is then given by

$$\Gamma_m(z) = c_{m,0}\Gamma_\perp(z) + (c_{m,-1} + c_{m,1})\Gamma_\parallel(z), \quad (7)$$

where  $c_{m,q}$  is shorthand for the square of a Clebsch-Gordan coefficient,  $c_{m,q} = \langle 2, m-q, 1, q | 3, m \rangle^2$ . Note that this implies that close to the surface the  $m$  states have different lifetimes [17]. The different  $\Gamma_m(z)$  curves are shown in Fig. 5, together with  $\Gamma_\perp(z)$  and  $\Gamma_\parallel(z)$ . The curve for  $|m| = 3$  is not relevant in our experiment because our  $p$ -polarized probe does not excite these  $m$ -states. Our  $^{87}\text{Rb}$  atoms are in a random mixture of all five  $|2, m\rangle$  states. The probe light is linearly polarized, perpendicular to the surface, thus exciting  $q = 0$  transitions.

## VI. ANALYSIS; COMPARISON WITH THEORY

Integrating the photon scattering rate  $\Gamma s/2$  over all  $z$  and averaging over the  $m$ -states, we arrive at the absorp-

tion of the probe; expressed as a fraction:

$$-\frac{\Delta P}{P} \propto \int_0^\infty \sum_{m=-2}^2 \frac{\Gamma_m(z) c_{m,0} \rho(z) e^{-2z/\xi}}{\delta_m^2(z) + \Gamma_m^2(z)/4} dz, \quad (8)$$

where  $\rho(z)$  is the atom density. It is  $z$ -dependent due to the ground-state level shift that accelerates the atoms to the surface. This is well approximated by the Van der Waals potential  $-C_3/z^3$ , resulting in a depletion of the density near the surface according to  $\rho(z) = \rho_0(1 + (z_W/z)^3)^{-1/2}$  with  $z_W = (C_3^g/mgh)^{1/3} \approx 50$  nm. Here  $C_3^g = 5.6 \times 10^{-49}$  J m<sup>3</sup> is the Van der Waals coefficient and  $mgh$  is the kinetic energy with which the atoms fall onto the surface.

The  $z$ -dependence of the laser detuning  $\delta_m(z)$  in Eq. (8) accounts for the energy level shifts by unequal amounts for the ground and excited states. The shift of the ground  $5S_{1/2}$  state is dominated by the Van der Waals shift  $-C_3^g/z^3$ . The shift of the excited  $5P_{3/2}$  state is more complicated, containing also a resonant component with oscillatory  $z$ -dependence. We have used expressions for the shifts of both the ground and the excited states from Ref. [16], using transition line strengths taken from Ref. [22]. We have extended the expressions from [16] to account for hyperfine structure. Furthermore we have multiplied the results by a factor  $(n^2 - 1)/(n^2 + 1)$ , because our surface is a dielectric instead of a mirror. This is known to be correct in the nonretarded limit [23], which gives the dominant contribution in the experiment.

It is evident from Eq. (8) that the absorption profile is a convolution of Lorentzians with different widths, amplitudes, and central frequencies. The resulting absorption profiles are strictly speaking no longer Lorentzian. We have numerically calculated the expected absorption profiles using Eq. (8). In practice the deviation from a Lorentzian is sufficiently small that we can fit a Lorentzian to the calculated profiles. The fitted widths are plotted in Fig. 4, together with the measured widths. In the same Figure we also show the result of the calculation if we do not take the level shifts into account. Clearly, the effect of the level shifts on the observed linewidth is comparable with the direct broadening effect.

From the Figure we also see that the observed broadening of up to about 25% is larger than the calculated broadening by about a factor two. This cannot be explained by the most obvious sources of spurious broadening. These include Doppler broadening (< 2%), Zeeman broadening due to a spurious magnetic field (< 3%), and power broadening (< 0.5%). Furthermore these broadening mechanisms do not show the observed signature of increasing with the angle of incidence. A drift of the laser frequency can be excluded by the same argument, plus the free-space data point.

A possible mechanism that would have the correct signature is transit time broadening. To investigate this we numerically integrated the time-dependent optical Bloch equations for an atom moving through the EW field. We

made the approximation that the atom is a two-level system. First, the known ground state level shift was used to solve for the accelerated motion  $z(t)$  towards the surface. This solution was then used to define a time-dependent Rabi-frequency  $\Omega_1(z(t)) = \Omega_{10} \exp(-2z(t)/\xi)$ , and similarly for the detuning  $\delta(z(t))$ , and radiative linewidth  $\Gamma(z(t))$ . Using these time dependent parameters we numerically integrated the optical Bloch equations to obtain the time evolution of the Bloch vector  $(u(t), v(t), w(t))$ . Note that power broadening is naturally included in this method. The number of photons scattered by the atom on its way down to the surface was obtained as  $\int \Omega_1(t)v(t)dt$  [24]. Again an averaging over the magnetic  $m$ -levels was performed. Finally the probe detuning was varied and a Lorentzian fit to the obtained absorption profile was performed, as before. The results of the Bloch equation approach are also shown in Fig. 4. The two calculations yield very similar results. This shows that transit time broadening does not explain the discrepancy between calculations and measurements.

As a tentative explanation we invoke the presence of local Stark shifts caused by charged or polarized particles on the surface. Based on a straightforward model calculation we find that a surface charge density of  $45e/\lambda^2$  yields a 10% linewidth increase. Remarkably, such a charge density corresponds to an average distance between the charges of order  $\sim 100$  nm, which is just the distance scale to which our experiment is very sensitive. These calculations only weakly reproduce the angular dependence shown by the data. Recently McGuirk *et al.* have reported that Rb adsorbed on a Si or Ti surface generates local Stark shifts that were measurable as a change in the trapping frequency of their magnetic trap [25]. The authors mention that similar effects on a glass surface like ours are very small. However, there may be other charged or polarized adsorbates on the surface. Our experiment is complementary to Ref. [25] in the sense that the latter measures a global effect, whereas our experiment is sensitive only to local variations of the electric fields. Unfortunately we have no detailed information about possible adsorbates to make a more quantitative analysis.

## VII. CONCLUSION

In conclusion, we have observed a broadening of the natural linewidth of the  $D_2$  resonance line of  $^{87}\text{Rb}$ . This broadening was a combined effect of QED linewidth broadening and level shifts due to the proximity of a dielectric surface. The observed broadening of up to 25% was about twice that expected from QED calculations. The most likely candidate to explain this discrepancy are local Stark shifts due to charged or polarized adsorbates on the surface.

## Acknowledgments

This work is part of the research program of the Stichting voor Fundamenteel Onderzoek van de Materie (Foundation for the Fundamental Research on Matter) and was made possible by financial support from the Nederlandse Organisatie voor Wetenschappelijk Onderzoek (Netherlands Organization for the Advancement of Research).

---

[1] E. A. Hinds, *Adv. At. Mol. Opt. Phys.*, Suppl. **2**, 1 (1994).

[2] K. H. Drexhage, *J. Lumin.* **1-2**, 693 (1970).

[3] K. H. Drexhage, in *Progress in Optics XII*, edited by E. Wolf (North-Holland, Amsterdam, 1974), p. 163.

[4] R. G. Hulet, E. S. Hilfer, and D. Kleppner, *Phys. Rev. Lett.* **55**, 2137 (1985).

[5] D. J. Heinzen, J. J. Childs, J. E. Thomas, and M. S. Feld, *Phys. Rev. Lett.* **58**, 1320 (1987).

[6] A. M. Vredenberg *et al.*, *Phys. Rev. Lett.* **71**, 517 (1993).

[7] E. Snoeks, A. Lagendijk, and A. Polman, *Phys. Rev. Lett.* **74**, 2459 (1995).

[8] V. Sandoghdar, C. Sukenik, E. Hinds, and S. Haroche, *Phys. Rev. Lett.* **68**, 3432 (1992).

[9] C. Sukenik *et al.*, *Phys. Rev. Lett.* **70**, 560 (1993).

[10] M. Chevrollier, D. Bloch, G. Rahmat, and M. Ducloy, *Opt. Lett.* **16**, 1879 (1991).

[11] H. Failache *et al.*, *Eur. Phys. J. D* **23**, 237 (2003).

[12] J. Eschner, C. Raab, F. Schmidt-Kaler, and R. Blatt, *Nature* **413**, 495 (2001).

[13] M. A. Wilson *et al.*, *Phys. Rev. Lett.* **91**, 213602 (2003).

[14] R. A. Cornelussen *et al.*, *Eur. Phys. J. D* **21**, 347 (2002).

[15] H. Khosravi and R. Loudon, *Proc. R. Soc. London A* **433**, 337 (1991).

[16] E. A. Hinds and V. Sandoghdar, *Phys. Rev. A* **43**, 398 (1991).

[17] J.-Y. Courtois, J.-M. Courty, and J. C. Mertz, *Phys. Rev. A* **53**, 1862 (1996).

[18] S.-T. Wu and C. Eberlein, *Proc. R. Soc. London A* **455**, 2487 (1999).

[19] D. Voigt *et al.*, *C. R. Acad. Sci. Paris, Série IV* **2**, 619 (2001).

[20] L. D. Turner, K. P. Weber, C. J. Hawthorn, and R. E. Scholten, *Opt. Commun.* **201**, 391 (2002).

[21] C. E. Wieman and L. Hollberg, *Rev. Sci. Instrum.* **62**, 1 (1991).

[22] M. S. Safronova, C. J. Williams, and C. W. Clark, *physics/0307057*.

[23] C. Eberlein and S.-T. Wu, *Phys. Rev. A* **68**, 033813 (2003).

[24] C. Cohen-Tannoudji, J. Dupont-Roc, and G. Grynberg, *Atom-photon interactions* (Wiley, New York, 1992).

[25] J. M. McGuirk, D. M. Harber, J. M. Obrecht, and E. A. Cornell, *cond-mat/0403254*.

[26] Note that there appears a printing error in Eq. (58) of [17]; the coefficients  $r^p(u)$  and  $r^s(u)$  have been interchanged.